Functional Role of Arginine-11 in the N-Terminal Helix of Skeletal Troponin C: Combined Mutagenesis and Molecular Dynamics Investigation†

Jagdish Gulati,‡ Arvind B. Akella,‡ Hong Su,‡ Ernest L. Mehler,§ and Harel Weinstein*,§

The Molecular Physiology Laboratory, Division of Cardiology, Departments of Medicine and Physiology/Biophysics, Albert Einstein College of Medicine, Bronx, New York 10461, and Department of Physiology and Biophysics, Mount Sinai School of Medicine, New York, New York 10029

Received December 29, 1994; Revised Manuscript Received March 31, 1995⊗

ABSTRACT: The two main structural differences between calmodulin (CaM) and skeletal troponin C (sTnC) are the absence in CaM of (i) the short N-terminal helix in TnC and (ii) the triplet KGK (residues 91−93; numbering according to chicken sTnC). It was recently shown that deletion of both structural groups from sTnC imparted to the resulting construct the CaM-like ability to activate phosphodiesterase (PDE) and to regulate force development in smooth muscle. To continue probing of the structural basis of the differential behavior of sTnC and CaM, residue Arg-11 in rabbit sTnC was mutated to Ala because the interactions of Arg-11 with distal residues in the N-terminal domain seem to link the N-terminal helix to the rest of the structure. The mutant exhibits CaM-like function in its ability to activate PDE (about 50% of CaM at 5 μM concentration). If, in addition, the KGK triplet is also deleted, PDE activation increases to about 80%. Both constructs retain their TnC function to nearly 100%. To explore the mechanistic basis of this remarkable observation, computational simulations of the molecular dynamics (MD) were carried out for both wild-type $4Ca^{2+}$•sTnC and the $4Ca^{2+}$•R11A mutant, and the results were compared to those from earlier simulations of $4Ca^{2+}$•CaM. Two types of structural changes observed from such simulations of the molecular dynamics of CaM had been considered to have a functional role: (i) a compaction to a more globular form and (ii) a reorientation of the Ca-binding domains around the central tether helix. Both changes occur in the experimentally determined structures of complexes of CaM with the CaM-binding peptides from myosin light chain kinase. The results of the MD simulations on sTnC showed that both the wild type and the R11A mutant compacted, but differently, so that reorientation of the N- and C-terminal domains was found only in the simulated structure of the mutant. Since the occurrence of both structural changes seems essential for the function of CaM, the simulations provide an explanation for the experimental observation that R11A, but not wild-type TnC, exhibits CaM-like behavior. In the structure of $4Ca^{2+}$•sTnC resulting from the simulation, R11 forms a structural link to the N-terminal domain via water-bridged hydrogen bonds. This link is absent in the R11A mutant, and the characteristics of the molecular and functional properties of the mutant indicate the mechanism by which the mutation induces properties required for CaM-like function in PDE activation.

The great variety of cellular processes controlled by Ca^{2+} ions involves specialized Ca-binding proteins that have evolved to execute regulatory or modulatory functions (Kawasaki & Kretsinger 1994). Troponin C (TnC)[1] and calmodulin (CaM) are among the best characterized regulatory proteins that are activated by changes in Ca^{2+} concentrations in the cell (McPhalen et al., 1991). These two proteins are highly homologous with similar secondary and tertiary structures (Weinstein & Mehler, 1994), but they have very disparate functional capabilities. Whereas CaM is a multifunctional Ca-dependent regulatory protein, TnC uniquely constitutes the Ca-dependent on/off switch in muscle contraction (Cohen & Klee, 1988; Zot & Potter, 1987). Consequently, several recent studies have used genetic manipulations to compare the structure−function relations of these proteins in efforts to explore the molecular basis of the Ca-dependent switching mechanisms (Brandt et al., 1994; Chandra et al., 1994; Gulati et al., 1993; Smith et al., 1994).

In the crystal, both CaM and TnC are dumbbell-shaped molecules, each comprising four repeats of the elements of supersecondary structure known as Ca-binding EF-hands. Two major structural differences between CaM and TnC are directly evident: One is the N-terminal helix that appears only in TnC, and another is a lysine−glycine−lysine sequence in the central helix of TnC that is not present in CaM [see Strynadka and James (1989)] (the KGK triplet, residues 91−93; the residue numbering scheme of chicken skeletal TnC is used throughout). The effect of deleting these two major structural differences from the TnC in rabbit skeletal muscle (sTnC) was investigated recently (Gulati et al., 1993). This double deletion TnC construct was found to mimic CaM in its ability to regulate force development

† Supported by the NIH (AR-33736, GM-41373, DA-00060), NY Heart Association Grant-in-Aid, and the Blumkin Fund.

* Address correspondence to this author [telephone (212) 241-7018; Fax, (212) 860-3369; e.mail, HWEINSTEIN @ MSVAX.MSSM.EDU].

‡ Albert Einstein College of Medicine.

§ Mount Sinai School of Medicine.

⊗ Abstract published in *Advance ACS Abstracts,* May 15, 1995.

[1] Abbreviations: CaM, calmodulin; TnC, troponin C; sTnC, skeletal TnC; cTnC, cardiac TnC; PDE, phosphodiesterase; SAXS, small-angle X-ray scattering; WT, wild type; Rg, radius of gyration; sk- or smMLCK, skeletal or smooth muscle myosin light chain kinase; VDA, virtual dihedral angle; MD, molecular dynamics; DTT, dithiothreitol; EGTA, ethylenebis(oxyethylenenitrilo)tetraacetic acid; EDTA, ethylenediaminetetraacetic acid; PAGE, polyacrylamide gel electrophoresis; pCa, $-\log [Ca^{2+}]$; Nt, N-terminal helix.

0006-2960/95/0434-7348$09.00/0

in smooth muscle, as well as in its activation of phosphodiesterase (PDE) in an enzymatic assay system *in vitro* (Gulati et al., 1993), even while preserving the capacity to govern contractile force development in skeletal muscle. However, the underlying mechanistic aspects of this remarkable functional transformation remain unknown. In the evaluation of these aspects at a structural level, the R11 residue stands out because it has been identified from the crystal structure of sTnC (Herzberg & James, 1988) as the only prominent contact of the N-terminal helix (Nt) with the rest of the molecule. These authors had noted a well-formed hydrogen bond between R11 and E76; a weaker H-bonding type interaction is indicated to E16 (Herzberg & James, 1988; Satyshur et al., 1994). These interactions establish a link of Nt to the entire N-terminal domain. However, the N-terminal domain of TnC is calcium free in the crystal structure (Herzberg & James, 1988), so that it is not clear to what extent the interaction between R11 and this domain is maintained in the functional fully Ca^{2+}-loaded structure. To study the role of R11 in the functional distinction between TnC and CaM, the mutation R11A was carried out in the Nt of sTnC, and the properties of the resulting construct were investigated as described here, using both experimental and computational methods.

The functional consequences of R11A mutations were evaluated with the measurements of PDE activity *in vitro*, as well as from an assay of the Ca regulation of force development in the skeletal myofiber. In parallel, molecular dynamics simulations were carried out on both wild-type (WT) and R11A sTnC to explore the molecular basis of the functional changes resulting from the mutations. Previous simulations of the dynamic properties of CaM and TnC (Mehler et al., 1991; Pascual-Ahuir et al., 1991; Weinstein & Mehler, 1992) have indicated that in solution the tether helix linking the two Ca-binding globular domains is highly flexible in CaM, allowing the domains to reorient and to come closer together. Like the results from small-angle X-ray scattering (SAXS) experiments (Heidorn & Trewhella, 1988; Heidorn et al., 1989; Kataoka et al., 1989, 1991; Matsushima et al., 1989; Seaton et al., 1985), the molecular dynamics simulations (Mehler et al., 1991; Pascual-Ahuir et al., 1991) suggested that the radius of gyration of the Ca^{2+}-loaded CaM structure is smaller than would appear from the X-ray structure (Babu et al., 1988). The simulations further showed that the propensity for compaction is less for TnC than for CaM and that any TnC compaction which does occur proceeds by a different mechanism compared to CaM (Mehler et al., 1991). Unlike CaM, which has been shown to be in a compacted conformation when bound to targets (Ikura et al., 1992; Meador et al., 1992), the function of TnC in muscle contraction seems to be independent of such compaction (Olah et al., 1994). The structural basis for this difference in the dynamic properties of the two molecules is therefore of considerable interest and can be elucidated from molecular dynamics (MD) simulations.

The mechanism of compaction in CaM suggested by the MD simulations involves a reorientation of the two globular Ca-binding domains. The two domains that point away from each other in the crystal structure are reoriented in the simulation. Their inner faces are repositioned so that they point toward each other in a manner that allows residues in both domains to interact with a helix in the protein target of CaM. The full significance of this reorientation of the lobes, concomitant with the structural compaction, became clear from the comparison of the NMR structure of the complex between CaM and the skMLCK target peptide (Ikura et al., 1992) to that of CaM alone in the crystal (Babu et al., 1988). In the structure of the complex, a segment of the helical tether had dissolved into a loop (residues 74−82), allowing the two domains to come closer together (the radius of gyration, Rg, is reduced to 17 Å as compared with 22 Å for CaM in the crystal structure) and to reorient in such a way that the inner faces of the domains interact with the target peptide like a clamp holding the latter in place (Ikura et al., 1992). A crystallographic study of CaM complexed with the target peptide smMLCK (Meador et al., 1992), which has a slightly different sequence than the target peptide of skMLCK, found very similar results. The segment of the tether which dissolved (residues 73−77) and the orientation of the domains in the complex were somewhat different from those in the CaM−skMLCK complex. Nevertheless, both studies clearly showed domain reorientation and compaction of the structure, as evidenced also in the simulations. The implications of this time-dependent flexibility, characteristic of CaM, for both its selectivity and its binding affinity for various targets have been discussed recently (Weinstein & Mehler, 1994). The inferences from the computed dynamic properties suggest that in complexes with different targets CaM will assume different orientations of the interacting interfaces.

In contrast to CaM, the function of TnC as an on/off switch for muscular contraction seems to depend on the precise separation between the two lobes during the complexation of TnC with TnI (Babu et al., 1993; Keleti et al., 1994; Olah & Trewhella, 1994). Therefore, the present comparative analysis of functional and molecular properties of WT sTnC and its variants centers on the properties that are likely to determine the differences between TnC and CaM in their mechanisms of interaction with targets.

METHODS

(A) Experimental Procedures

(1) Mutagenesis. The mutants were generated from the cDNA encoding rabbit fast-twitch skeletal muscle TnC, as described previously (Babu et al., 1993; Babu et al., 1992). The gene was cloned in the pT7 plasmid and included 22 unique restriction sequences which greatly facilitated the mutagenesis. The proteins were expressed in *Escherichia coli* (DE3-pLysS cells, Novagen) under the specific induction of IPTG. The purification of bacterially synthesized proteins was carried out by column chromatography as before [Babu et al., 1992; see also Xu and Hitchcock-DeGregori (1988)]. Each protein was checked by SDS−PAGE for purity and produced a single band with characteristic Ca dependency [Figure 1; see also Gulati et al. (1992)]. The protein concentration was determined with the Bio-Rad protein assay kit using a TnC standard (Gulati et al., 1993).

Two constructs were engineered: In the R11A mutant, arginine-11 in Nt was mutated to alanine, using polymerase chain reaction. Cassette mutagenesis was used to generate a double mutant in which the KGK triplet of residues was deleted as well. The other mutants, designated ΔNt and ΔNt·ΔKGK, were the same as described before (Gulati et al., 1993). The wild-type recombinant protein is termed sTnC4 to distinguish it from the tissue sTnC.

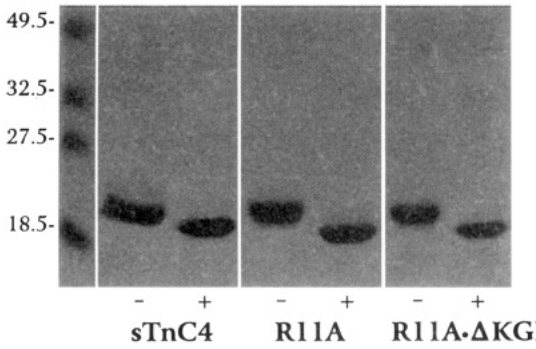

FIGURE 1: Ca-dependent mobilities of WT sTnC4 and its variants R11A and R11A·ΔKGK on 12% SDS−polyacrylamide gels: (−), EGTA; (+), Ca^{2+}. The first lane indicates the molecular mass standards between 18.5 and 49.5 kDa.

(2) Ca^{2+}-Binding Potentials. Measurements of maximal Ca^{2+} binding by the new proteins were made by equilibrium microdialysis in saturating free Ca^{2+} solutions (pCa 3.5) using radiolabeled $^{45}Ca^{2+}$, as described in Gulati et al. (1992). Forty-eight hour dialysis at 4 °C was used throughout. The wild-type sTnC4 was included for these measurements as a control.

(3) Permeabilized Rabbit Psoas Fibers: TnC Extraction and Reconstitution. Muscle fiber segments, typically 50−150 μm wide and 2−4 mm long, were isolated from the rabbit muscle and permeabilized as described earlier (Gulati, 1976; Gulati et al., 1991). The fiber was attached between a transducer and the free arm of a servomotor, and the fiber length was kept small to help maintain sarcomere uniformity during activation. The sarcomere length following attachment was adjusted at 2.5 μm in the relaxing solution and was monitored frequently with laser diffraction during the experiment.

The effects of the TnC mutants on the fiber were assessed by first extracting the endogenous TnC and then repleting the extracted fiber with a desired mutant. As before (Babu et al., 1987; Gulati et al., 1991), the TnC extraction was carried out in an EDTA solution (5 mM K_3EDTA, 10 mM imidazole, pH 7.2) at 28 °C. The maximally Ca^{2+}-activated tension following extraction was typically below $0.05P_0$ (P_0 = maximal tension of the same skinned fiber prior to extraction). Maximal Ca^{2+} activations of the rabbit fibers were routinely done at 5 °C.

For TnC repletion, the extracted fiber was superfused for 5 min in the *relaxing* solution [20 mM imidazole, 6.5 mM ATP, 5 mM EGTA, 15 mM phosphocreatine, 6 mM $MgCl_2$, 90 mM potassium propionate, pH 7.0, 5 °C; 180 mM ionic strength; modified from Gulati and Podolsky (1978)] containing approximately 1 mg/mL mutant TnC or wild-type TnC (sTnC4), and then the fiber was incubated in the relaxing solution without the protein to wash out any free protein. Subsequently, activation was induced with 100 μM Ca^{2+} (pCa 4). The TnC repletion was repeated and the force level compared with the first. If the force level in the repeat cycle was within 1−2% of that in the first cycle, no further repletion was attempted. The final assurance regarding completion of the loading of the particular protein was derived from quantitative analyses of polyacrylamide gel electrophoresis (SDS−PAGE) developed from selected experimental fiber segments, as described previously (Ding et al., 1994).

(4) Phosphodiesterase (PDE) Activation with the TnC Derivatives. To compare the efficacy of the mutants to that of CaM, the competencies of the proteins (at 5 μM concentrations) to activate the PDE enzyme for hydrolysis of cAMP into AMP was determined *in vitro* in a cascade reaction as described before (Gulati et al., 1993). The value for CaM was taken as 100%.

(B) Computational Procedures

(1) Model Structures. The starting model of fully Ca^{2+}-occupied TnC was constructed from the available crystal structure (Herzberg & James, 1985, 1988), which contains only two Ca^{2+} in the C-terminal domain, using the proposal by Herzberg et al. (1986) that the tertiary configuration of the helices and loops of the N-terminal domain will shift to resemble those in the fully occupied C-domain. Molecular modeling of the TnC resulted in a structure of the N-terminal domain (residues 15−83) with an RMS deviation of 3.96 Å (RMS differences are based on the superpositioning of Cα) from the X-ray coordinates [cf. the RMS of 4.05 Å reported by Herzberg et al. (1986)]. The RMS difference between the N- and C-terminal domains of the model was 0.94 Å (N-domain, residues 19−83; C-domain, residues 95−159). The RMS deviation of the modeled N-terminal domain from the corresponding region in the N-terminal domain of the crystal structure of CaM (residues 5−73) was only 1.70 Å.

The tertiary structure of the model N-terminal domain of TnC obtained from this procedure is thus reasonably close to that reported previously (Herzberg et al., 1986), and is even closer to that found in CaM, but is substantially different from that of the apo domain in the crystal of TnC. Replacement of R11 by alanine in this model of fully Ca^{2+}-loaded TnC provided the starting structure for the R11A mutant. All subsequent steps in the computational simulations described below were identical for both the WT protein and the mutant.

(2) Molecular Dynamics Simulations. To prepare the two structures for simulation, they were immersed in a 4 Å shell of solvent molecules with the SOAK option of the InsightII graphics software (Biosym), implemented on a Silicon Graphics platform. The complete systems, consisting of the WT or R11A protein, four Ca^{2+} ions bound in the binding loops of the EF hands, and 916 water molecules, comprised 4417 and 4406 atoms, respectively. The 4 Å shell of water molecules provides only a minimal solvent model that would not be appropriate to carry out a full characterization of the system, but earlier simulations have shown that this reduced solvation model is adequate for investigating the global structural changes of interest in this study (Mehler et al., 1993).

All further calculations were carried out with the CHARMM program package (Brooks et al., 1983) (version 22) with unit dielectric constant using the united atom model and the PAR19 parameter set with default values for the control parameters. The SHAKE algorithm (van Gunsteren & Berendsen, 1977) was used to constrain the X−H bond lengths, and a time step of 1 fs was used in the simulations. For minimization the nonbonded list was updated every 25 steps, but for the simulations the update was carried out every 10 steps.

The model structures were energy minimized in two steps: First the water shell was optimized with the protein

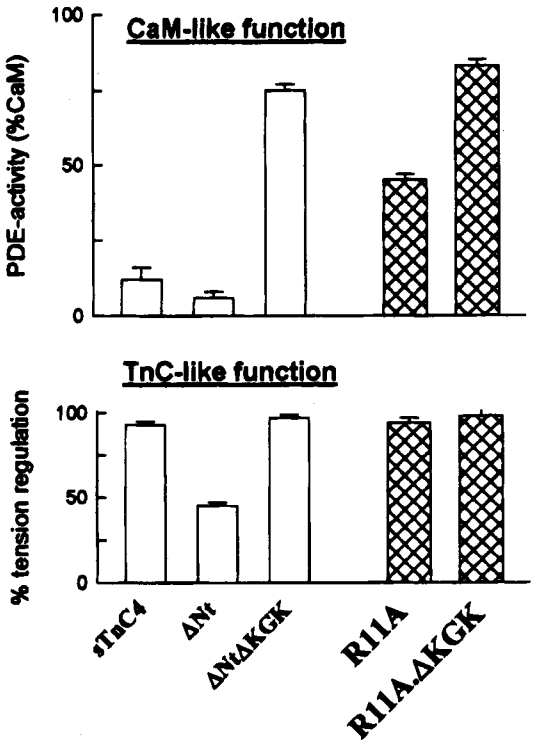

FIGURE 2: Functional characterizations of the R11A mutants of rabbit sTnC. (The numbering corresponds to chicken sTnC, which contains three additional residues in the N-terminus.) The upper panel shows the CaM-mimetic performance of R11A and R11A·ΔKGK mutants by PDE-activity measurements *in vitro*. All values are normalized to CaM. The lower panel shows activity of the constructs in the Ca regulation of force development. All these values are normalized to native skinned fiber containing endogenous sTnC. The data for sTnC4, ΔNt, and ΔNt·ΔKGK indicated by open bars are similar to those in Gulati et al. (1993).

and Ca^{2+} coordinates held fixed, and then the entire system was relaxed. The energy-minimized structures were used to equilibrate the water shells by again fixing the proteins and Ca^{2+} coordinates, heating the solvent shells to 300 K, and equilibrating the solvent for 50 ps. The last structure in each trajectory (i.e., snapshots of WT sTnC and R11A at 50 ps) was then reminimized, and the resulting coordinates provided the starting structures for the simulations. Each system was heated to 300 K in 6 ps, and the simulations were then continued until the trajectories stabilized, as determined from the RMS differences between the simulated and starting structures of the domains. For structural comparisons, average structures were extracted from the trajectories (250−400 ps for WT sTnC and 200−350 ps for R11A) and energy minimized to remove unphysical interatomic distances.

RESULTS AND DISCUSSION

(A) CaM-like Activity of the R11A Mutants. To gain insights into the functional role of R11, the PDE stimulatory activities of the mutant constructs were compared to those of wild-type CaM and TnC. Figure 2 indicates the performance of various proteins in both the *in vitro* PDE assay and fiber force development. The data for PDE activities were normalized to the value for saturating CaM, and the data for tension were normalized to the force level of the unextracted fiber in saturating Ca (pCa 4). As noted above (Methods), the ΔNt and ΔNt·ΔKGK mutant constructs assayed in addition to the R11A and R11A·ΔKGK constructs described here were the same as before (Gulati et al., 1993).

Table 1: Ca^{2+}-Binding Potential of Different Proteins

protein	mutation	Ca^{2+} binding (mol/mol of protein)
sTnC4	bacterially synthesized wild-type	3.92 ± 0.03 (12)
R11A	Arg (residue 11) in the N-helix converted to Ala	3.84 ± 0.03 (6)
R11A·ΔKGK	R11A with concomitant deletion of KGK triplex in the central helix	3.93 ± 0.07 (6)

The PDE measurement indicates that the R11A mutants have significant CaM-like activity, unlike the wild-type sTnC4 or the mutant (ΔNt) in which the N-helix had been deleted. Nevertheless, both R11A mutants retained normal TnC function in their force development capability in maximally activated skinned fibers (Figure 2). The maximal Ca-binding capability of these mutants was also normal (4 mol/mol of protein), as shown in Table 1. Moreover, as indicated in Figure 1, characteristic Ca^{2+}-dependent mobilities were also indistinguishable between wild-type sTnC4 and the R11A mutant. The acquisition by the R11A construct of both TnC- and CaM-like functions is indicative of intrinsic conformational versatility, as discussed below.

(B) Structure and Dynamics of WT and R11A sTnC. The flexibility observed for CaM can be characterized by two variables representing compaction and interdomain orientation, respectively. The former is most conveniently obtained from the radius of gyration (Rg) while a measure of the latter is given by the virtual dihedral angle (VDA) defined from the positions of the four bound Ca^{2+} ions from the N-terminal EF-hand to the C-terminal EF-hand (see inset, Figure 3). For the crystal structures of CaM and TnC the values of this angle are 226° and 183°, respectively, whereas for the CaM−skMLCK complex the value is 109°. (The dihedral angles are expressed in the interval 0−360° with 0° defined as in the IUPAC (1970) convention.) The structures resulting from the simulations of CaM reported earlier (Mehler et al., 1991; Pascual-Ahuir et al., 1991) cluster at VDA values around 26° and 290°. Notably some degree of reorientation of the N- and C-terminal domains was observed in all these structures as a concomitant of compaction, thus expressing the structural consequences of the flexibility implied from the results of the NMR study of CaM (Barbato et al., 1992).

The Cα RMS differences of the N- and C-terminal domains in the starting structure and in the average, minimized structures obtained from the MD simulations of the WT protein and R11A mutant are all ≤1.5 Å. Such small differences indicate that the secondary and tertiary structures within the domains are well preserved during the simulation, in spite of the significant changes in the structure of the central helix as evidenced by the radii of gyration (Rg) of the molecules: At the start of the simulation (after heating to 300 K) the Rg of the WT and R11A proteins were 22.8 and 22.9 Å, respectively. At 300 ps into the trajectory, the Rg were 18 and 19 Å for WT sTnC and R11A, respectively, which represents a significant difference. Interestingly, continuation of the trajectory of R11A to 470 ps resulted in an Rg value of 18 Å, close to the value for WT sTnC. In comparison, the final Rg value for CaM was 17 Å, but there the rate of compaction was shown to vary between 100 and

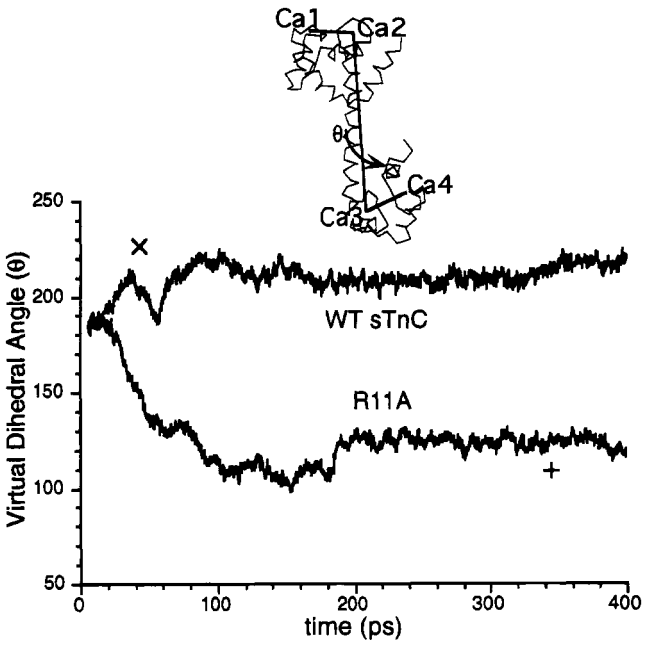

FIGURE 3: Time evolution of the virtual dihedral angle between the four Ca^{2+} ions, measured from the N-terminal EF-hand to the C-terminal EF-hand. The inset defines the virtual dihedral angle (VDA), θ, connecting the four Ca^{2+} ions. Note that for ease of plotting the standard IUPAC (1970) convention for measuring dihedral angles has been changed to the interval 0−360°. × denotes the VDA value in the crystal structure of CaM (Babu et al., 1988); + indicates the VDA value for CaM in the CaM−skMLCK complex (Ikura et al., 1992).

600 ps, depending on the starting conditions for the simulation (Pascual-Ahuir et al., 1991). The disparities in the compaction rates between WT sTnC and R11A observed here may be due to the different compaction mechanisms followed by the two systems as indicated below.

As discussed previously (Mehler et al., 1991) the compacted state found here after several hundred picoseconds of dynamics represents only one component of the equilibrium between extended and compacted structures that are accessible to these proteins (Barbato et al., 1992). Results from both SAXS studies (Heidorn & Trewhella, 1988; Heidorn et al., 1989) and from the NMR studies of CaM (Barbato et al., 1992) have suggested a dynamic partitioning between compacted and extended conformations in solution. This partitioning is compatible with the interpretation of the MD simulation results in terms of a time-averaged pair distribution function $P(r)$, which can be expressed (Mehler et al., 1991) as a linear combination of the pair distribution functions for the extended $[P_{ext}(r)]$ and the compacted forms $[P_{comp}(r)]$:

$$P(r) = \alpha P_{ext}(r) + (1 - \alpha)P_{comp}(r)$$

Mehler et al. (1991) obtained an expression for the weighting coefficient, α, and found a value of 0.71. Using this value of α, the calculated distribution function was in excellent agreement with the observed $P(r)$ [cf. Figure 8C in Mehler et al. (1991) and Figure 3B in Matsushima et al. (1989)], indicating the relation between the MD simulation results and the experimental evidence for dynamic transitions between compacted and extended structures of CaM.

The conservation of secondary and tertiary structures of the globular N- and C-terminal domains in the present simulations of WT sTnC and R11A is in agreement with observations from the NMR studies of CaM (Barbato et al., 1992) and from the complex of CaM with the skMLCK target peptide (Ikura et al., 1992). However, in the final structures of R11A the reorientation of the domains was quite different from that in WT sTnC. At the start of the simulation, the VDA between the four Ca ions was about 183° for both, but as shown in Figure 3, the WT protein reoriented only slightly with time to a final value of 208°. In contrast, the domains in the mutant were substantially reoriented to a final value of 121°, which is close to the value noted above for CaM−skMLCK. Therefore, *the R11A mutant, but not WT sTnC, exhibits both characteristics associated with CaM-like behavior: domain reorientation and compaction.* Moreover, the value of the VDA achieved by R11A suggests that the inner faces of the two domains reorient during the simulation to a position more conducive to CaM-like complex formation.

Because of the crucial differences in the average structure of WT sTnC and R11A, the dynamics of compaction of R11A must also be reflective of the structural alterations in the tethering helix. These are evident in Figure 4, which compares both structures to a simulated structure of CaM (Mehler et al., 1991). Comparison of the tether helix (colored in blue) in the three structures shows that the bends in R11A and in CaM involve corresponding residues. In contrast, the central region of the tether helix in TnC is relatively straight, and the position of the bend is shifted much closer to the N-terminal domain. Interestingly, the bend in R11A is located on the C-terminal side of the KGK triplet (shown in magenta in Figure 4), whereas in WT sTnC, the bend is seen to be on the N-terminal side of KGK (Figure 4). Thus it appears that the compaction seen in the WT protein proceeds by a path different from that in the R11A mutant, which is much more similar to that of CaM. The difference between WT sTnC and CaM is consistent with earlier observations from simulations using a simpler solvation model (Mehler et al., 1991).

The role of R11 in determining the observed differences between WT sTnC and the R11A mutant may relate to the interaction of R11 with E76 observed in the crystal structure as well as its weak interaction with E16 (Herzberg & James, 1988; Satyshur et al., 1994). These interactions link the N-terminal helix to the first residue (E16) of helix A and the second residue (E76) of helix D, so that the connections to R11 span the domain. In the initial model of the Ca^{2+}-loaded structure ($4Ca^{2+}$·TnC), the distances between the proton donor (R11) and the proton acceptors have increased from 3.1 and 3.8 Å for E76 and E16, respectively, as observed in the crystal structure, to around 5 Å. In the average structure of WT sTnC obtained from the molecular dynamics trajectory, these H-bonds have not been reestablished, but one finds a rich network of interactions between R11 and water comprising at least ten water molecules within 3.5 Å of one of the two guanidine nitrogens. Both E16 and E76 are bridged to R11 by two (occasionally one) of these waters. Since this water-bridged array forms hydrogen bonds between charged groups, the interactions are quite strong, although not as strong as the direct H-bond between the charged species R11 and E76. The time-dependent behavior of this system of persistent water-bridged H-bonds suggests a continuous exchange of the bridging water molecules with the bulk solvent. Together with the smaller binding energies

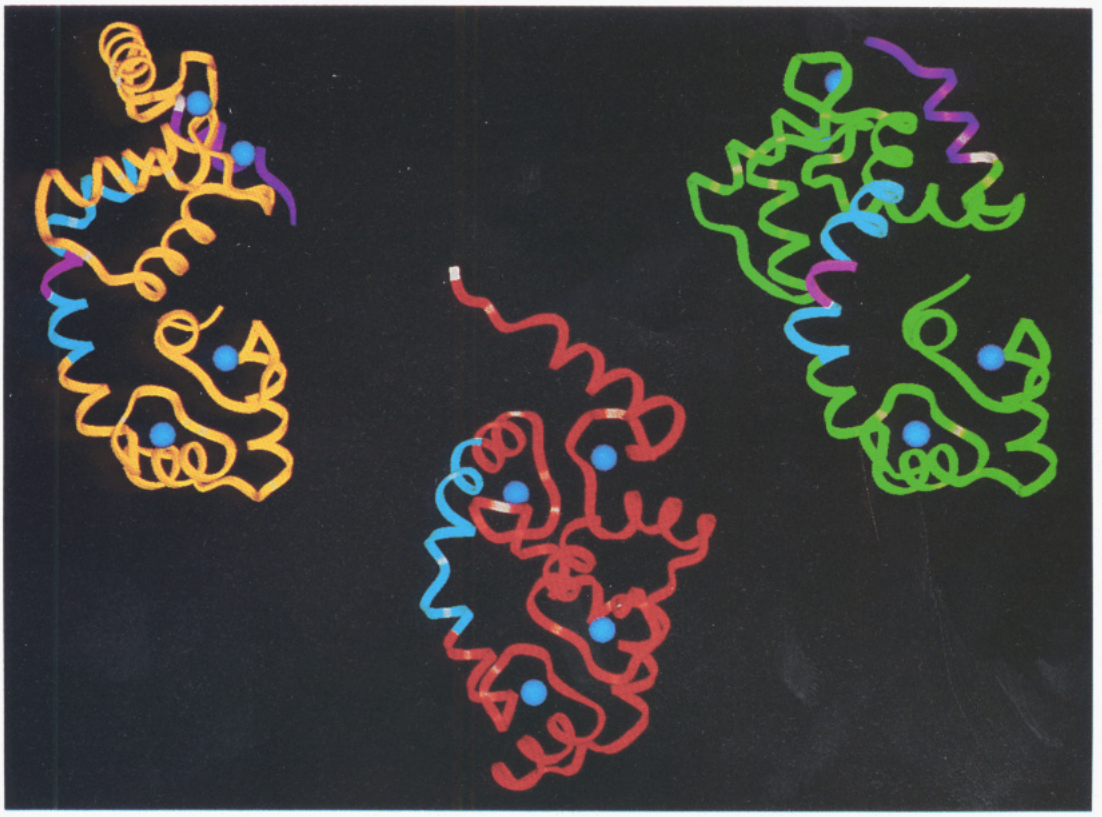

FIGURE 4: Ribbon diagrams of simulated molecular structures for WT sTnC (yellow), R11A (green), and CaM (red) (Mehler et al., 1991). Nt is shown in purple, residue 11 (1 in CaM) is in white, the tethering helix (residues 82−98 in TnC and residues 72−85 in CaM) is in blue, and KGK is colored magenta in WT sTnC and the R11A mutant. To obtain similar orientations for all three structures, the C-terminal domains of WT sTnC and R11A were superimposed on the C-terminal domain of CaM.

of these H-bonds, the solvent exchange implies greater motional freedom, i.e., flexibility, for the entire domain compared to that obtainable if direct H-bonding of R11 to E76 and (more weakly) to E16 were observed. The flexibility acquired in this fashion by the Ca-loaded N-terminal domain may be essential for the binding of the target protein. Conversely, removal of Ca^{2+} from the two binding sites in the domain would reestablish the rigid bonds formed by R11 and thus diminish further the probability of interaction with the target. In the R11A mutant these interactions are absent, eliminating the structural link between the protein regions containing the arginine (R11) and the two glutamic acids (E16 and E76). Notably, position 11 in TnC corresponds to the first residue of CaM, so that the mutation R11A renders this position identical to the N-terminal residue of CaM.

(C) Structural Determinants of the CaM-like Activity of the TnC Mutants. In addition to the CaM-like dynamic properties, the ability of the present TnC mutants to perform CaM-like activation of PDE probably has its origin in their high sequence homology to the regions identified from CaM target complexes to be involved in the interaction surfaces. The sequence identities of the N- and C-terminal domains of CaM with skeletal TnC (Strynadka & James, 1988) are 56% and 27%, respectively. However, if in each domain one selects only the 19 residues in loci found in CaM to be involved in interactions with the target peptide of skMLCK (Ikura et al., 1992), these identities increase to 84% and 58% for the two domains, respectively. Thus, especially the N-terminal domain of TnC could act like its corresponding domain in CaM if the overall structural rearrangement were feasible.

A comparison of the N- and C-terminal domains of the simulated structures with the observed structures of CaM in the crystal and in the complex with skMLCK reveals that the N-terminal domains of the two experimental structures of CaM exhibit a substantially larger difference than the C-terminal domain (see Table 2). This implies that the N-terminal domain is more affected by the interaction with the target peptide. The same ordering was also found for the RMS differences between the two experimental structures of CaM and the simulated structures of WT sTnC and R11A. The RMS values reported in Table 2 also show that both domains of R11A differ less from the crystal structure of CaM than the corresponding domains of WT sTnC, indicating the greater similarity of the mutant to CaM. When compared to CaM from the CaM−skMLCK complex, only the C-terminal domain of R11A is closer to CaM, but the RMS differences calculated from the snapshots (Table 2, values in parentheses) show that at times the increased similarity also occurs for the N-terminal domain of R11A. Since no structural information from CaM is used in defining the simulation protocols of either WT skTnC or R11A, it is tempting to conclude from the simulations that the additional flexibility imparted by the mutation allows the mutant protein to mimic the structural dynamics of CaM.

The bioassays showed that deletion of the KGK triplet in the R11A construct further increased the functional similarity of the mutant to CaM in PDE activation (Figure 2). Thus, it is likely that the presence of the KGK triplet in WT sTnC

Table 2: RMS (Å) Differences between Domains of CaM and TnC

	CaM (X-ray)[a]		CaM (NMR)[b]	
	N[c]	C[d]	N[c]	C[d]
CaM (NMR)[b]	1.97	1.54		
WT sTnC[e]	2.22 (2.21)	1.86 (1.40)	3.04 (3.24)	2.35 (1.86)
R11A sTnC[f]	2.07 (1.94)	1.33 (1.22)	3.22 (2.97)	1.86 (1.61)

[a] CaM X-ray Structure (Babu et al., 1988). [b] Solution structure of CaM complexed with target peptide of skMLCK (Ikura et al., 1992); RMS in angstroms. [c] N-Terminal domain: CaM, residues 5−73; TnC, residues 15−83. [d] C-Terminal domain: CaM, residues 83−147; TnC, residues 96−160. [e] sTnC wild-type structure; values represent RMS differences for the average simulated structures (see text); numbers in parentheses are from 203 ps snapshot. [f] sTnC mutant Arg-11 to Ala; values represent RMS differences for the average simulated structures (see text); numbers in parentheses are from 198 ps snapshot.

affects the two essential attributes of the central helix dynamics, i.e., deformation and domain reorientation, in ways that enhance the observed functional differences between CaM and TnC. This hypothesis is currently being explored with further computational simulations. Interestingly, the original TnC-like function is retained by these mutants, indicating that the enhanced central helix dynamics render the mutants functionally less restrictive than either the wild-type TnC or CaM.

CONCLUDING REMARKS

The present analysis of the structural basis for CaM-like activity of TnC mutants shows that in the Ca^{2+}-occupied N-terminal domain, R11 interacts with both proximal and distal regions (i.e., E16 and E76) in the N-terminal domain via water-bridged hydrogen bonds. This interaction is different from that observed in the apo domain, where R11 comes closer to the E16 and E76 residues (Herzberg & James, 1988; Satyshur et al., 1994) and forms stronger interactions that provide structural rigidity. Because Ca^{2+} occupancy seems to be a determinant factor in this interaction between structural elements of Nt and the rest of the TnC molecule, it is attractive to suggest that R11 is part of a dynamic Ca-dependent structural link between the N-terminal helix and the rest of the protein. In the absence of the link provided by R11, the mutant sTnC acquires more pronounced CaM-like properties. On the other hand, the importance of this essential communication, which is modified in the R11A mutant, for TnC-like function is suggested by the observation that Nt is crucial for sTnC function both in the regulation of Ca^{2+}-dependent contractility in the skinned fiber (Ding et al., 1994; Gulati et al., 1993; Smith et al., 1994; Chandra et al., 1994) and in the regulation of Ca^{2+}-sensitivity in the isolated protein (Chandra et al., 1994; Rao, Akella, Su, and Gulati, unpublished).

The manner in which structural properties contribute to the observed CaM-like properties of R11A is clarified by the results of the present computational simulations that revealed both the CaM-like flexibility and the similarity of the structural rearrangement resulting from the different dynamic properties of the R11A mutant compared to WT sTnC. Although an Arg is consistently found at the corresponding structural position of all known vertebrate sTnCs, it is noteworthy that in cardiac TnC R11 is replaced by a valine. It is not clear if structural differences in the cardiac EF-hand of site 1 render the requirement for R11 less critical for achieving differentiation from CaM. Whether this is the case, or whether valine has a functional role that is specific to the cardiac TnC function, needs to be investigated in further studies.

Finally, the multifunctional aspect of CaM activity seems to relate to its ability to acquire a variety of conformations that match the appropriate target structures (Mehler & Weinstein, 1994). Thus, the question of whether or not the present R11A construct can exhibit comparable multifunctionality is an interesting one for further exploration [e.g., by studying the smooth muscle activation; see Gulati et al. (1993)].

ACKNOWLEDGMENT

Computational support was provided by the Pittsburgh Supercomputer Center (sponsored by the National Science Foundation), the Cornell National Supercomputer Facility (sponsored by the National Science Foundation and IBM), the Advanced Scientific Computing Laboratory at the Frederick Cancer Research Facility of the National Cancer Institute (Laboratory for Mathematical Biology), and the University Computer Center of the City University of New York.

REFERENCES

Babu, A., Scordilis, S., Sonnenblick, E., & Gulati, J. (1987) *J. Biol. Chem. 262*, 5815−5822.
Babu, A., Su, H., Ryu, Y., & Gulati, J. (1992) *J. Biol. Chem. 267*, 15469−15474.
Babu, A., Rao, V. G., Su, H., & Gulati, J. (1993) *J. Biol. Chem. 268*, 19232−19238.
Babu, Y. S., Bugg, C. E., & Cook, W. J. (1988) *J. Mol. Biol. 204*, 191−204.
Barbato, G., Ikura, M., Kay, L. E., Pastor, R. W., & Bax, A. (1992) *Biochemistry 31*, 5269−5278.
Brandt, P. W., George, S. E., & Schachat, F. (1994) *FEBS Lett. 353*, 99−102.
Brooks, B. R., Bruccoleri, R. E., Olafson, B. D., States, D. J., Swaminathan, S., & Karplus, M. (1983) *J. Comput. Chem. 4*, 187−217.
Chandra, M., McCubbin, D., Oikawa, K., Kay, C. M., & Smillie, L. B. (1994) *Biochemistry 33*, 2961−2969.
Cohen, P., & Klee, C. B., Eds. (1988) *Calmodulin*, Elsevier Press, Amsterdam.
Ding, X.-L., Akella, A. B., Su, H., & Gulati, J. (1994) *Protein Sci. 3*, 2089−2096.
Gulati, J. (1976) *Proc. Natl. Acad. Sci. U.S.A. 73*, 4693−4697.
Gulati, J., & Podolsky, R. J. (1978) *J. Gen. Physiol. 72*, 701−715.
Gulati, J., Sonnenblick, E. H., & Babu, A. (1991) *J. Physiol. 441*, 305−324.
Gulati, J., Babu, A., & Su, H. (1992) *J. Biol. Chem. 267*, 25073−25077.
Gulati, J., Babu, A., Su, H., & Zhang, Y.-F. (1993) *J. Biol. Chem. 268*, 11685−11690.
Heidorn, D. B., & Trewhella, J. (1988) *Biochemistry 27*, 909−915.
Heidorn, P. B., Seeger, P. A., Rokop, S. E., Blumenthal, D. K., Means, A. R., Crespi, H., & Trewhella, J. (1989) *Biochemistry 28*, 6757−6764.
Herzberg, O., & James, M. N. G. (1985) *Nature (London) 313*, 653−659.
Herzberg, O., & James, M. N. G. (1988) *J. Mol. Biol. 203*, 761−779.
Herzberg, O., Moult, J., & James, M. N. G. (1986) *J. Biol. Chem. 261*, 2638−2644.
Ikura, M., Clore, G. M., Gronenborn, A. M., Zhu, G., Klee, C. B., & Bax, A. (1992) *Science 256*, 632−638.
IUPAC (1970) *Biochemistry 9*, 3471−3479.
Kataoka, M., Head, J. F., Seaton, B. A., & Engelman, D. M. (1989) *Proc. Natl. Acad. Sci. U.S.A. 86*, 6944−6948.
Kataoka, M., Head, J. F., Vorherr, T., Krebs, J., & Carafoli, E. (1991) *Biochemistry 30*, 6247−6251.

Kawasaki, H., & Kretsinger, R. H. (1994) *Protein Profile 1*, 343−517.
Keleti, D., Rao, V. G., Su, H., Akella, A. B., Ding, X.-L., & Gulati, J. (1994) *FEBS Lett. 354*, 135−139.
Matsushima, N., Izumi, Y., Matsuo, T., Yoshino, H., Ueki, T., & Miyake, Y. (1989) *J. Biochem. 105*, 883−887.
McPhalen, C. A., Strynadka, N. C. J., & James, M. N. G. (1991) *Adv. Protein Chem. 42*, 77−144.
Meador, W. E., Means, A. R., & Quiocho, F. A. (1992) *Science 257*, 1251−1255.
Mehler, E. L., Pascual-Ahuir, J. L., & Weinstein, H. (1991) *Protein Eng. 4*, 625−637.
Mehler, E. L., Kushick, J. N., & Weinstein, H. (1993) *Mol. Simul. 10*, 309−334.
Olah, G. A., & Trewhella, J. (1994) *Biophys. J. 66*, A311.
Olah, G. A., Rokop, S. E., Wang, C.-L. A., Blechner, S. L., & Trewhella, J. (1994) *Biochemistry 33*, 8233−8239.
Pascual-Ahuir, J.-L., Mehler, E. L., & Weinstein, H. (1991) *Mol. Eng. 1*, 231−247.
Satyshur, K. A., Pyzalska, D., Greaser, M., Rao, S. T., & Sundralingam, M. (1994) *Acta Crystallogr. D50*, 40−49.
Seaton, B. A., Head, J. F., Engelman, D. M., & Richards, F. M. (1985) *Biochemistry 24*, 6740−6743.
Smith, L., Greenfield, M. J., & Hitchcock, S. E. (1994) *J. Biol. Chem. 269*, 9857−9863.
Strynadka, N. C. J., & James, M. N. G. (1988) *Proteins: Struct., Funct., Genet. 3*, 1−17.
Strynadka, N. C. J., & James, M. N. G. (1989) *Annu. Rev. Biochem. 58*, 951−998.
van Gunsteren, W. F., & Berendsen, H. J. C. (1977) *J. Mol. Phys. 34*, 1311−1327.
Weinstein, H., & Mehler, E. L. (1992) in *Molecular Aspects of Biotechnology: Computational Models and Theories* (Bertran, J., Ed.) pp 153−173, Kluwer Academic Publishers, Dordrecht, The Netherlands.
Weinstein, H., & Mehler, E. L. (1994) *Annu. Rev. Physiol. 56*, 213−236.
Xu, G.-Q., & Hitchcock-Degregori, S. E. (1988) *J. Biol. Chem. 263*, 13962−13969.
Zot, A. S., & Potter, J. D. (1987) *Annu. Rev. Biophys. Biophys. Chem. 16*, 533−559.

BI943008S